Max-Planck-Institut
für Meteorologie

REPORT No. 96

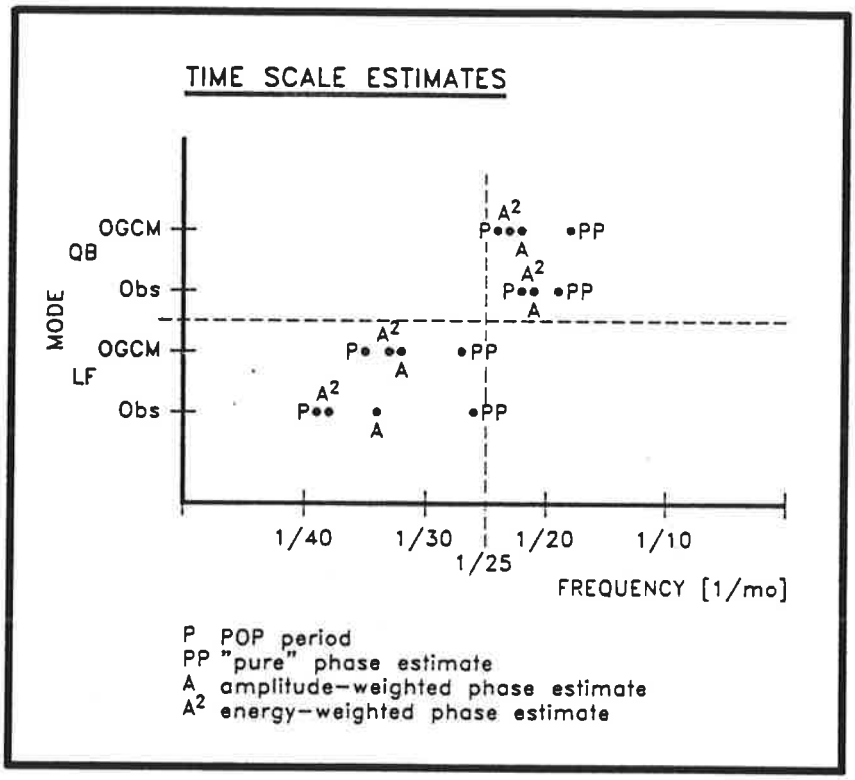

MODAL STRUCTURE OF VARIATIONS IN THE TROPICAL CLIMATE SYSTEM
PART II: ORIGINS OF THE LOW-FREQUENCY MODE

by

TIMOTHY P. BARNETT • MOJIB LATIF
NICHOLAS E. GRAHAM • MORITZ FLÜGEL

HAMBURG, DECEMBER 1992

AUTHORS:

Mojib Latif
Moritz Flügel

Max–Planck–Institut
für Meteorologie

Timothy P. Barnett
Nicholas E. Graham

Climate Research Division
Scripps Institution of Oceanography
La Jolla
California 92093
U.S.A.

MAX–PLANCK–INSTITUT
FÜR METEOROLOGIE
BUNDESSTRASSE 55
D–2000 HAMBURG 13
F.R. GERMANY

Tel.: +49 (40) 4 11 73–0
Telex: 211092 mpime d
Telemail: MPI.METEOROLOGY
Telefax: +49 (40) 4 11 73–298

REPb 96

MODAL STRUCTURE OF VARIATIONS IN THE TROPICAL CLIMATE SYSTEM PART II: ORIGINS OF THE LOW-FREQUENCY MODE

T.P. Barnett [1]

M. Latif [2]

N. Graham [1]

M. Flügel [2]

[1] Climate Research Division, Scripps Institution of Oceanography, La Jolla, CA

[2] Max Planck Institut fur Meteorologie, Hamburg, Germany

November 17, 1992

ISSN 0937–1060

Abstract

Simulations with ocean and atmospheric general circulation models and a hybrid coupled model reproduce well the observed features of variability in the low frequency (LF) mode described in Part I.

The model results show the origins of the LF to be in the ocean and suggest this phenomenon is a natural mode of the tropical Pacific Basin. Air-sea interactions amplify the ocean mode by a factor of 5-6 so it obtains climatological importance. These same interactions introduce the LF to the atmosphere. The physical processes responsible for these results are presented.

The LF mode of interannual variability is not directly driven by the annual cycle. But it does depend importantly on the fact that the ocean-atmosphere coupling strength vary with respect to the annual cycle. The LF mode appears to be rather sharply peaked in wave number space but broadbanded in frequency space.

1.0 Introduction

In the first part of this paper (Latif, *et al.*, 1993; hereafter Part I) we investigated and described three fundamental frequencies of variability in the ocean-atmosphere system of the tropical Pacific Ocean. These frequencies were defined objectively by a simultaneous Principal Oscillator Pattern (POPs) analysis* of the observed fields of wind stress, sea surface temperature (SST) and ocean heat content. The periods resulting from this analysis were roughly 12, 22 and 34 months. The first time scale was simply the annual cycle. Of the latter two time scales, the one near 34 months is the one of interest in this study. It has been shown to be a fundamental constituent of the El Niño-Southern Oscillation (ENSO) phenomenon (see below). We will refer to it here as the LF mode. The goal of the present paper is to determine the physical origins of this important mode of variation in the tropical climate system.

As was shown in Part I, the subsurface memory of the Tropical Pacific Ocean seems to play a crucial role in creating the LF mode. For convenience, we show the LF mode obtained from observations (interpolated to our ocean model grid) in Figure 1. The LF mode was shown to be consistent with the 'delayed action oscillator' scenario of Schopf and Suarez (1988) (see also Graham, and White (1988); Philander (1990); Cane *et al.*, (1990)). The time scale of the LF mode, however, is still a controversial issue. We have argued in Part I that the time scale of the LF mode is of the order of about 30 months, and this relatively short time scale was shown to enable non-linear interactions between the annual cycle, the quasi-biennial (QB), and the LF mode. Please note that in earlier work the term 'LF mode' referred to time scale of order 4-6 years (Ropelewski *et al.*, 1992; Barnett, 1991). Those earlier works referred to the mode with period around 30 months as 'the QB mode.' The QB mode we described in Part I has a time scale of about 22 months. This confusing situation is due to the fact that we are dealing with broadband processes. As already pointed out in Part I, estimates of time scales are, therefore, subject to large uncertainties. We address this issue further in Section 6. The important point, however, is that two modes of interannual variability exist in the tropical Pacific which have different spatial characteristics.

In this paper we use a series of model simulations to try to understand the origins of

* The POPs analysis allows at least four different ways of estimating a characteristic time scale. We present only one period here for simplicity. The variability associated with the different time scale estimation techniques is discussed in Section 6.

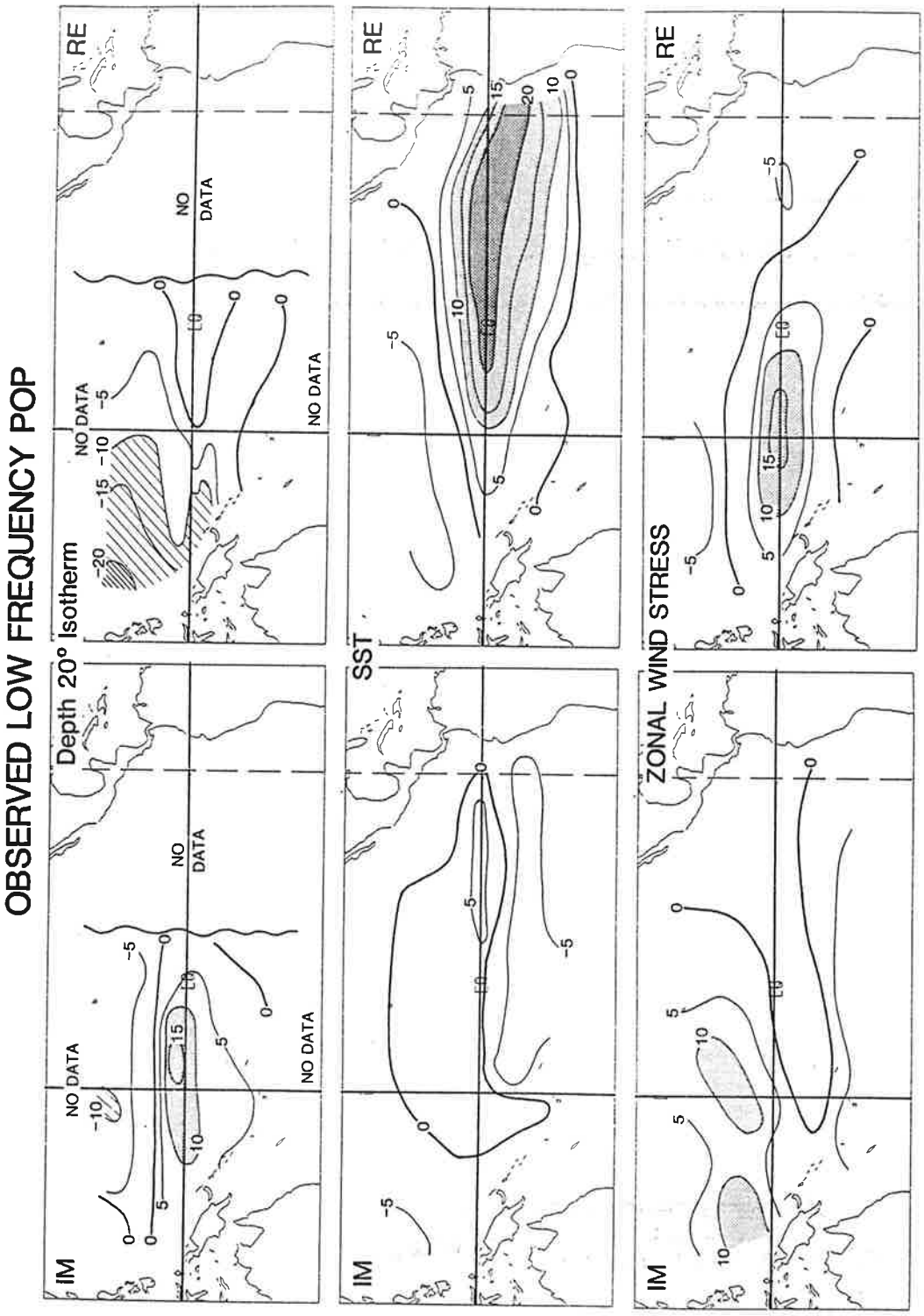

Fig. 1. Low-frequency (LF) POP mode as derived from a simultaneous POP-analysis of observed nondimensionalized heat content, SST, and zonal wind stress anomalies (top to bottom). The left panels show the imaginary patterns, the right panels the real part patterns (reproduced from Latif, *et al.*, (1993)). No heat content data was available over much of the Pacific Basin. The sense of the POPs is that the Real POP follows the Imaginary Pop by one quarter of a cycle.

the LF variations and the role of the seasonal cycle, if any, in its generation. This modeling work is complimentary to the observed data analysis of Part I. In the next section, we use a series of Atmospheric General Circulation Model (AGCM) runs and data to see if the LF is most likely of oceanic or atmospheric origin. In subsequent sections, we evaluate the ability of an ocean model driven with observed and random winds to reproduce the leading CEOF results obtained from the observations of Part I, and then use this ocean model in a coupled mode to investigate further the physics of the LF variability.

2.0 Possible Atmospheric Origins of the LF Mode

In this section we investigate the possibility that the LF signal originates in the atmosphere. The principal tool for this study is the ECHAM2 atmospheric general circulation model developed at the Max Planck Institute for Meteorology in Hamburg. The model has T21 resolution, 19 levels in the vertical, prognostic cloud water and a variety of other state-of-the-art features in its physics package. The model is more fully described in Fischer (1987), von Storch (1988) and Sausen (1991).

Two numerical experiments were conducted. The first was a 20-year control run in which the model was forced by seasonally varying insolation and sea surface temperature (SST), i.e., climatology. In the second experiment, the model was additionally forced by the observed global SST anomalies over the period 1970-88, a 19-year integration. This is referred to as the GAGO experiment and is described in more detail elsewhere (Latif, *et al.*, 1990; Barnett, *et al.*, 1991). A number of basic fields from both of these runs were analyzed. The general results obtained are illustrated below using the sea level pressure (SLP) field. The physical interpretations given were derived from the model physics fields.

The SLP fields from the GAGO run and the control run were band passed filtered to concentrate on the frequency band of interest, i.e. 20-40 months. Prior analysis (Barnett, 1991) showed that the majority of the energy in this filtered field was in the tropical Pacific and so the data fields were constrained to this region. The resulting filtered, decimated fields were then subjected to complex empirical orthogonal function (CEOF) analysis. The details of the CEOF method are given in Barnett (1983, 1991). In addition to the model SLP fields, we also performed a similar filtering and CEOF analysis on the observed SLP field in the region of interest over the time period 1970-88.

The results of all three CEOF studies are shown in Fig 2. The upper part of the illustration shows the leading CEOF obtained from the observations. This mode accounts for 70% of the variance in the filtered, area-limited data set. The clockwise rotation of the complex eigenvectors (plotted in polar form) in the equatorial zone, shows a signal that propagates from the Indian Ocean/western Pacific region eastward to South America. This signal in the CEOF is much like the Southern Oscillation and has been extensively described previously (Barnett, 1983, 1985a, 1991). The middle panel is the leading CEOF from the GAGO run and represents 59% of the variance in the SLP field from that anomaly run. The upper two panels have a complex pattern correlation whose modulus is 0.81, while their

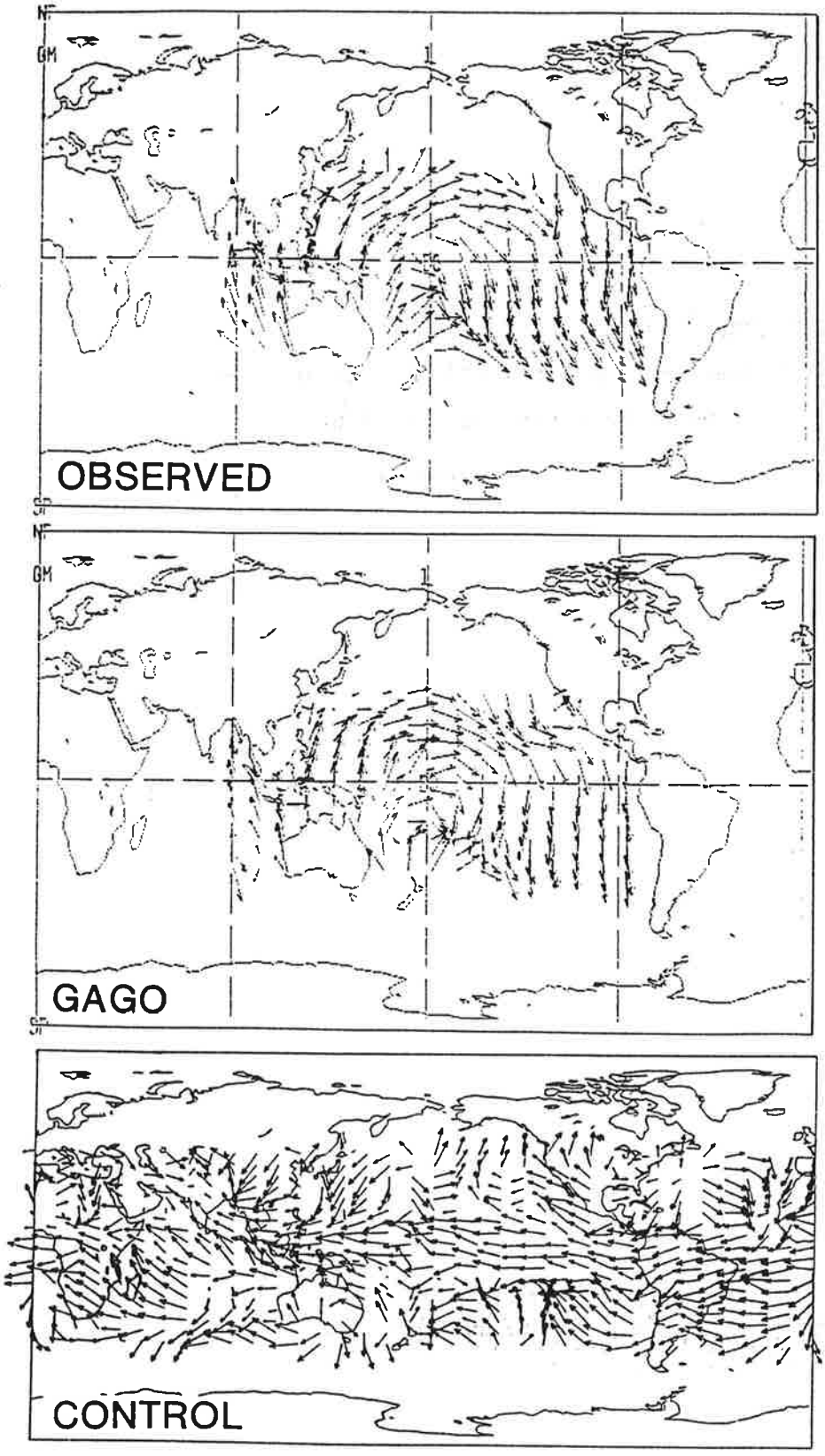

Fig. 2. Leading complex empirical orthogonal functions of the tropical sea level pressure field for the observations (upper), AGCM forced by observed SST (middle) and AGCM control run (lower). The data has been put through a band pass filter to emphasize the LF frequency band prior to analysis. The percent variance associated with each panel is given in the text.

associated principal components correlate at 0.96. Both numbers exceed the 0.01 significance level. The spatial pattern correlation, especially, represents a striking agreement between model and observation.

The lower panel of Fig. 2 shows the leading complex eigenvector from the control run (44% of the variance). A slightly larger domain is shown to emphasize the fact that the leading CEOF from the control run in no way resembles the structures seen in the GAGO run and the observations. The same is true for the higher CEOF modes of the control run. This strongly suggests that the atmosphere by itself cannot generate LF variability like that observed. Since the only difference between the two AGCM runs was the addition of SST anomaly information in the GAGO run, we conclude that the LF signal is fundamentally introduced by the ocean. We discuss later the degree to which the LF signal is an "ocean only" phenomenon as opposed to a closely coupled large scale air-sea interaction.

Examination of the model physics showed why the AGCM responded as it did. The atmospheric response is due to large scale equatorial precipitation anomalies that result from a shift of the main convection region eastward into the central Pacific during warm events...just as observed in nature. The principal mechanism driving the precipitation is the large scale, near-surface wind convergence associated with the anomalous SST gradients. The resulting moisture flux convergence then directly forces the precipitation. The anomalous moisture for the precipitation is not derived locally from evaporation but rather advected to the equatorial zone from the broad expanse of the Trade Winds. This physical scenario was just the one found to operate during warm extremes of the ENSO cycle (Barnett, *et al.*, 1991).

In summary, the numerical simulations suggest quite strongly that the LF mode under discussion has its origins in the oceans, not the atmosphere. This result does not preclude the possibility that air-sea interactions may play an important role in the LF. Indeed, we shall see below that such interactions are critical to the LF as it is observed in Nature and widely accepted in the relevant literature.

3.0 The LF Mode in an Ocean Model

Prior to using a series of ocean general circulation model (OGCM) experiments to dissect the physics of the LF mode, we first wish to demonstrate that the OGCM can reproduce the observed features of the LF described in Part I. The OGCM to be used in this study is the

nonlinear primitive equation version of the Hamburg tropical Pacific Ocean model (Latif, 1987) that calculates the three-dimensional current field, sea level and SST. The model has realistic horizontal geometry with a zonal grid spacing of 670km and a meridional resolution of 50km near the equator, expanding to about 400km at the northern/southern boundaries (30N/30S). There are thirteen irregularly spaced levels in the vertical, with ten of the levels in the upper 300m. Vertical mixing is accomplished through use of a Richardson's number dependent formalism. In the experiments to be described below, the model was forced with the observed, monthly FSU windstress for the period 1962-1990 (cf. Goldenberg and O'Brien, 1981). This simulation reproduced fairly well the observed broad-band SST variations over the period of interest (Miller, *et al.*, 1992).

The SST, sea level and wind stress fields resulting from the above model run were analyzed in exactly the same manner as were their observational counterparts (Part I). There were only two meaningful interannual POPs modes that resulted from this analysis, and they had periods of 24 and 35 months, respectively. Both of these values are remarkably close to the interannual values found in Part I. The first mode will be referred to as the QB mode and the last one as the LF mode. The spatial POP pattern associated with the LF mode is shown in Figure 3. It bears a close resemblance to the LF POP pattern found from the observations; compare with Figure 1. The degree of similarity was quantified by computing the complex pattern correlation between the (complex) LF POP from the data and the forced model run, i.e., between Figure 1 and Figure 3. The modulus of this correlation, which is a measure of the pattern correlation between the POPs, was 0.77. The temporal correlation of the associated (complex) POPs coefficients was 0.65, a value we would have expected from the earlier model evaluation of Miller *et al.*, 1992. In short, the model forced by the observed winds has done a reasonable job of reproducing the temporal evolution and spatial structure of the LF mode found in the observations.

We also investigated the degree of nonlinear coupling between the various POP modes in the forced OGCM run (see Barnett, 1991, or Part I for a description of the approach). The interaction coefficient for the triplet $< LF\ LF\ QB^{*} >$ had a value of 0.46, while the coefficient for the interaction of the triplet $< LF\ QB\ AC^{*} >$ was 0.65, both significant values at the 0.05 level. The interaction between the annual cycle (AC) and the QB or LF modes by themselves was insignificant. These results agree well with those of Part I both numerically and with regard to interpretation (see Part I, Section 4 for the appropriate discussion). The

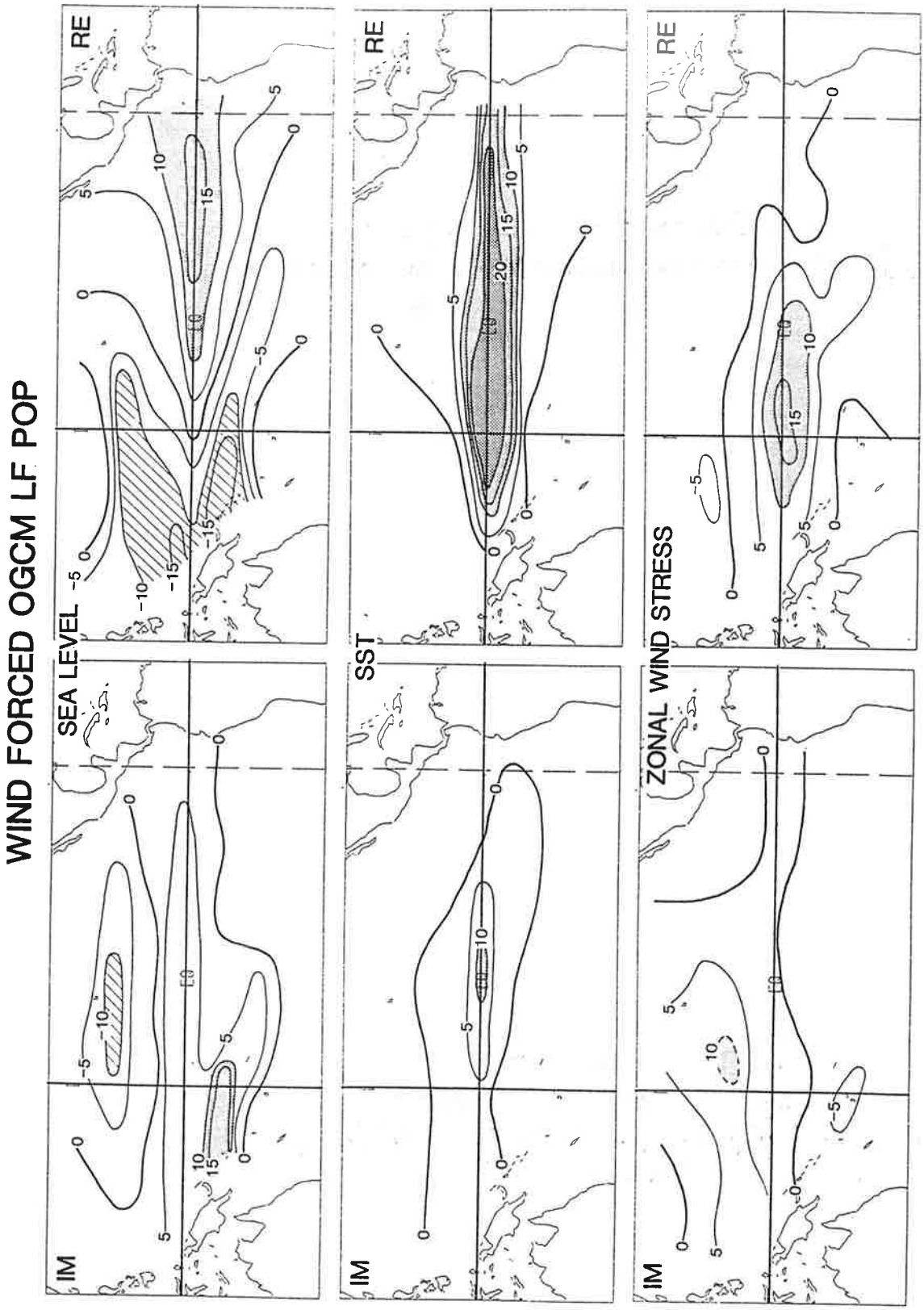

Fig. 3. Principal oscillator pattern (POP) for the LF mode obtained from the OGCM forced by 29 years of observed wind stress. This POP was derived from the multivariate field of sea level (upper), SST (middle), and zonal wind stress (lower). See Fig. 1 legend.

model results also agree in both respects with those obtained by Barnett (1991).

In summary, the OGCM forced by the observed winds has reproduced the LF mode results obtained from observations in Part I. It seems safe to conclude that the OGCM will be an adequate tool with which to pursue further simulations of the LF mode variability.

4.0 Oceanic Origins

In this section we investigate two ideas. The first is that the LF signal under discussion is a natural mode of the Pacific Basin, i.e., is a creature of oceanic origin. Second, we wish to see if such a mode results from an interaction of the annual cycle with itself. The answers to both questions were obtained from two simulations with the OGCM, each of which was 50 years in length. In the first simulation, the model was forced with the annual cycle of wind stress plus "noise". The noise was given by

$$N(\underline{x},t) = \sum_{i=1}^{10} a_i(t) e_i(\underline{x})$$

where $e_i(\underline{x})$ is the i^{th} empirical orthogonal function of the FSU anomalous wind stress data set (1965-88) and $a_i(t)$ is a random principal component constructed such that

$$a_i(t_n) = r_n(o, \lambda_i)$$

where r_n is the n^{th} random number drawn from a population with zero mean and variance λ_i, i.e., variance proportional to the i^{th} eigenvalue from the wind stress EOF analysis. Thus the forcing field of the anomalous wind stress was constructed to be "red in space and white in time".* We will refer to this experiment as the "annual cycle/noise" or ACN forced run. The second experiment is identical to the first, but now the seasonal cycle of wind forcing was replaced at each gridpoint by the annual average stress appropriate to that grid point. We refer to this experiment as the "annual average/noise" or AAN run. The same set of random numbers was used in each run to clearly delimit the role of the annual cycle in the experiments.

* In principal, a 'white-white' forcing should give the same result as the 'red-white' forcing but would require a far longer integration time to pull the signal from the noise. Since we expected any coupling to be associated only with the largest space scales, the choice of a 'red-white' forcing seemed both reasonable and economical.

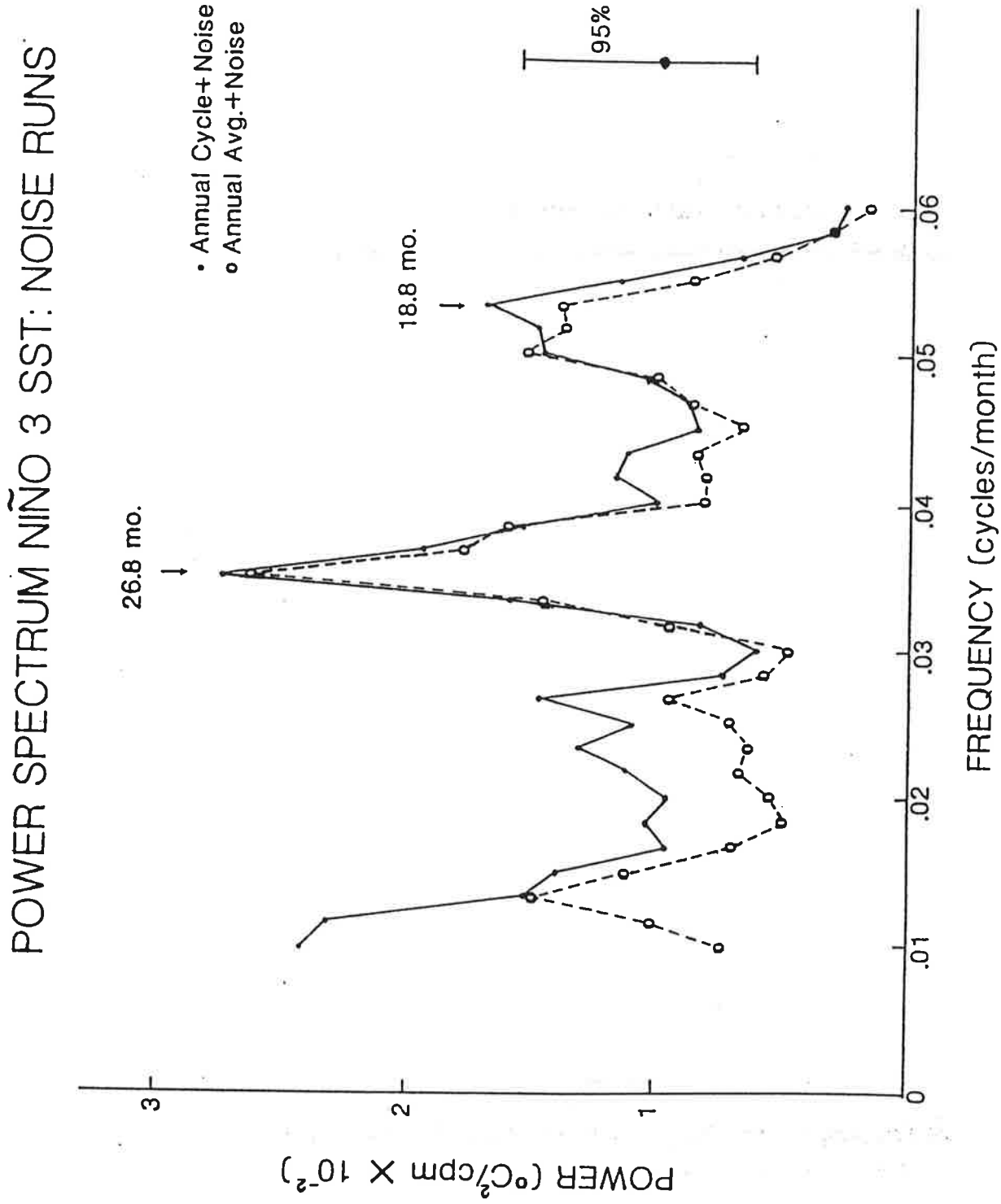

Fig. 4. Power spectra of NINO3 SST anomaly from 50-year OGCM runs forced by spatially red and temporally white anomalous wind stress. One run also included the regular seasonal cycle of wind stress (solid dot), while the other used annual average stress as climatological forcing (open circle). The NINO3 region is between 90-150W and 5N-5S.

The two numerical experiments are summarized succinctly in Figure 4 which shows the power spectrum of the SST anomaly for region NINO3 for each run. The illustration leads to two major conclusions:

i) The power spectra show a major peak at 26.8 months period and a secondary peak near 19 months. The lower frequency peak is significant, but the higher frequency peak is only marginally meaningful. The POP analysis of the white noise forced OGCM run produced an unstable periodicity, using the standard POP estimate, that varied between 24 and 29 months depending on the length of record used. The spatial patterns from this POP (Fig. 5) were quite similar to those obtained for the LF mode derived from the wind forced run from the OGCM (Section 3.0); the associated pattern correlation was 0.82. In addition, the POP pattern correlation between the white noise forced OGCM run and the comparable observed POP from Part I (Fig. 1) was 0.77. In essence then, the principal mode of the white noise forced run was the LF mode described above and in Part I. The 10-15% difference in time scale estimates is within the uncertainty of the individual estimates although we cannot show this rigorously (cf. Section 6).

The results strongly suggest that the LF variation is a natural mode of the Pacific Basin. This mode is oceanic in origin and apparently resonantly excited by the noise forcing imposed on the model. This, in turn, suggests the LF seen in these experiments is the result of ocean dynamics. We know of no theory that predicts the existence of such a time scale.

ii) The power spectra are nearly identical over the frequency range of interest, so the inclusion of the annual cycle (ACN), or the lack thereof (AAN), had little to do with variability outside its immediate frequency band. Thus the idea that the LF variations are somehow forced directly by the annual cycle, e.g., are a simple subharmonic of the annual cycle, is not supported by the numerical simulation. We repeated the ACN experiment for another realization of the white noise forcing and obtained essentially the same result as shown on Figure 4.

The very low frequency behavior of the model seen in the spectra is spurious. It arises from a slow drift associated with the lack of a long term balance in the heat budget of the model. This is induced largely by the model's failure to properly compensate for heat which should (in nature) be transported meridionally by the ocean but cannot be due to the solid "walls" at 30°N/S. Apparently the combination of diffusion and pseudo-heat flux parameterizations are not quite energy conserving over the model domain. This problem

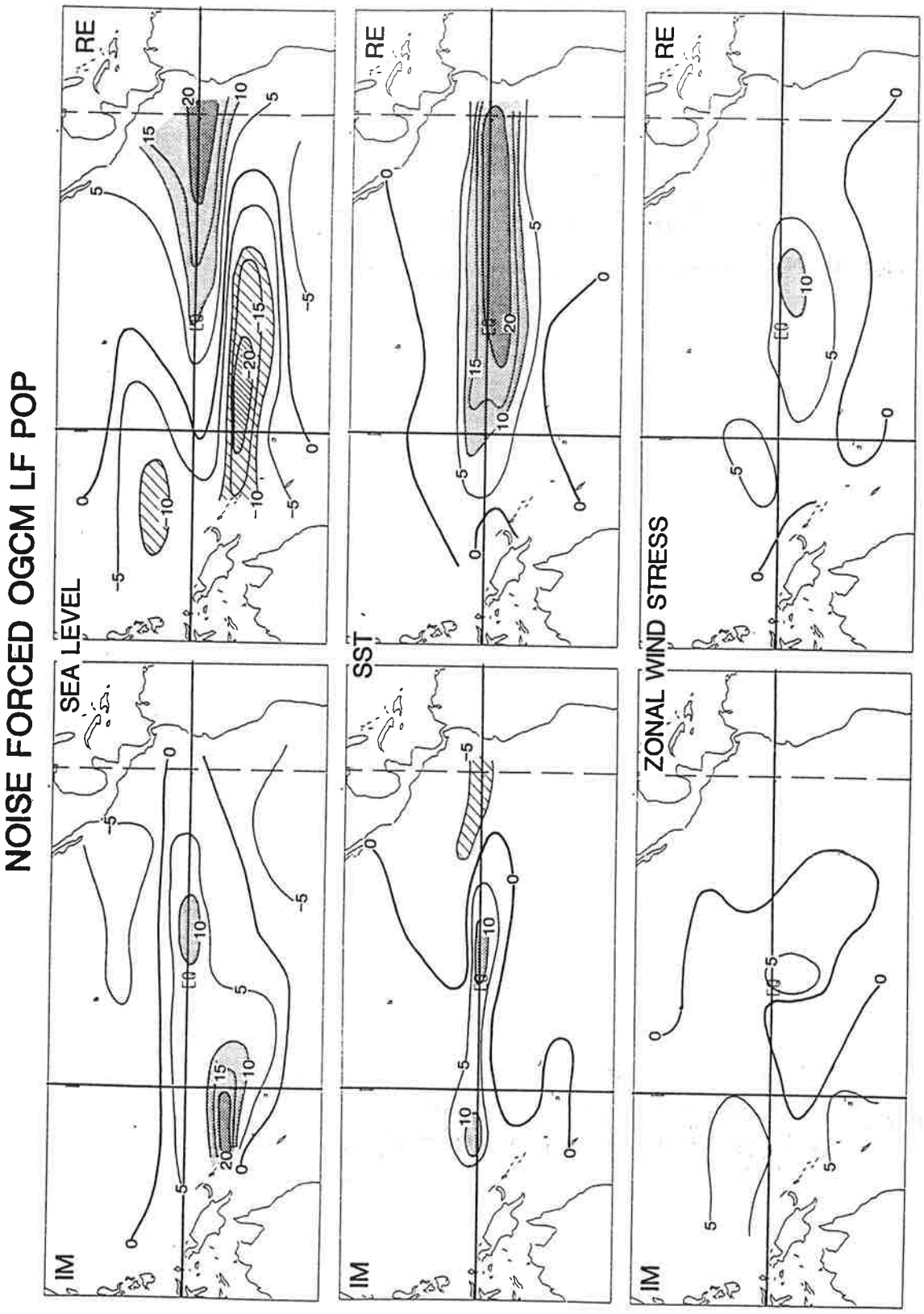

Fig. 5. As Fig. 3, but from the OGCM forced by wind stress that is 'red' in space and 'white' in time.

should have no impact on the use of the OGCM for ENSO-related studies.

In summary, the LF mode that is the subject of this paper seems to be a natural mode of the tropical Pacific Ocean. In the experiments reported here, this mode is excited by wind stress anomalies that are white in time but have the large scale spatial structure observed in nature. The simulations suggest that the annual cycle, by itself, has little or no role in directly forcing the LF variations we have found in the OGCM.

5.0 The Role of Ocean-Atmosphere Coupling

In this section we investigate the role of ocean-atmosphere coupling in the LF mode. The results from the preceding section would, at first glance, appear to rule out such a coupling, but this is not the case. The random wind field used in the above experiments is theoretically composed of an infinite number of Fourier components having different frequencies, wave numbers and directions of propagation. Thus, in analogy to the resonant theory of wind wave generation of Phillips (1962), there will be some element of the forcing field that could move and resonantly interact with the ocean features that comprise the LF mode.

The principal tool we will use in the following discussion is the hybrid coupled model (HCM) described by Barnett, *et al.*, (1993, hereafter B93). The ocean component of the HCM consists of the OGCM used in the earlier sections of this paper. The atmospheric component is a statistical model that specifies the anomalous windstress from information on anomalous SST provided by the ocean model. In effect, the atmosphere in the HCM is driven only by the local SST and SST gradients. The seasonal cycle for ocean variables is computed by the OGCM, while the seasonal cycle of atmospheric forcing is specified; the atmospheric model is thus an anomaly model. A critical element of the atmospheric model is that the ocean-atmosphere coupling coefficients were computed independently for each month of the year. It was shown in B93 that the HCM did a reasonable job of reproducing both the space and temporal variability observed in the ocean and atmosphere of the tropical Pacific. It also produced reasonable forecasts of large ENSO events at lead times out to 18 months in advance. In short, the HCM appears an adequate tool for studying the LF type of phenomenon.

5.1 HCM and the LF Mode

The HCM had a chaotic behavior, but showed a definite preference in extended integrations for oscillation at or near periods of two or three years. As noted in B93, the spatial

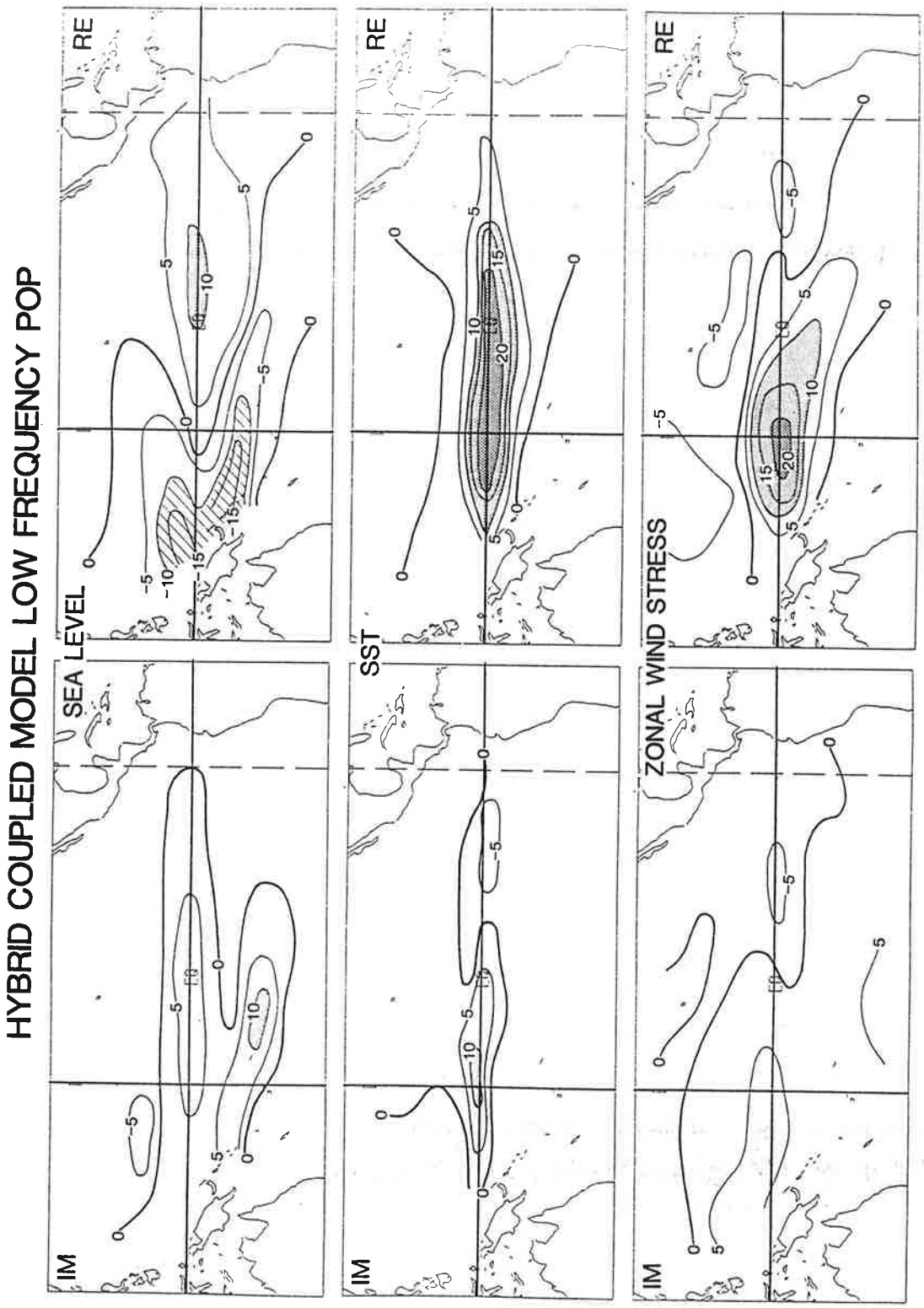

Fig. 6. POP associated with the LF frequency band in the hybrid coupled model (HCM). The analysis was performed on a multivariate data set composed of SST, sea level and zonal wind stress from a 50-year run of the HCM. See Barnett, *et al.* (1993) for more details on the model and associated analysis.

structure of this behavior was very similar to that observed in both the real SST and sea level fields independent of whether the HCM was oscillating at 2 or 3 year periods. This is partially illustrated in Figure 6. It is also important to note that the POPs results referred to in that illustration bear a marked similarity to those obtained from analysis of the 29-year integration of the OGCM forced by the observed winds (Section 3). The pattern correlation between the LF POPs from the wind forced run and a 50 year segment of HCM run was 0.84. Comparing the HCM POP with that derived from the observations yields a pattern correlation of 0.60 (between Figures 6 and 1). We conclude that the spatial response of the HCM is much like that seen in nature and in the wind forced OGCM (at least the LF mode).

Of interest here is the magnitude of the temporal variability of the HCM. During a 150-year control run, the model produced a 31-year sequence where NINO3 SST varied irregularly but with mean period of about 22 months (Epoch 1). From year 32 to 104 the model produced a quasi-biennial oscillation (Epoch 2), and after year 104 a triennial oscillation (Epoch 3). We concentrate here on Epoch 2, the period of biennial variations. As noted above, the spatial characteristics of the variability didn't change significantly from epoch to epoch. Specifically, we wished to see if the direct coupling between ocean and atmosphere in the HCM produced a stronger LF mode than was simulated in the noise runs just discussed. Prior to doing this comparison, we verified that the first and second EOFs of the HCM wind stress field compared well with observations, and that the level of anomalous stress variance was similar between the HCM model and the noise experiments of the previous section.

The power spectrum of NINO3 SST from a 50 year long section of Epoch 2 of the HCM control run (Fig. 7) showed a sharp peak at approximately a two-year period (as expected). This was slightly higher frequency than that found in the noise runs, but the above pattern correlation plus a separate analysis (B93) showed it is the HCM's equivalent of the LF signal. It is the magnitude of the peak that is of interest here. The details of the spectral analysis (record length, band width, smoothing, etc.) were the same as those used to produce Figure 4. The peak of the HCM spectrum was about 30 times higher than that in the noise run. We got about the same result from using a 50 year segment of Epoch 3. We infer from the more energetic HCM spectrum that air-sea interactions are helping to amplify the LF signal that naturally resides in the ocean. The physical mechanisms responsible for this amplification were explained in B93. Based on the relative magnitudes of the spectral peak energies (30

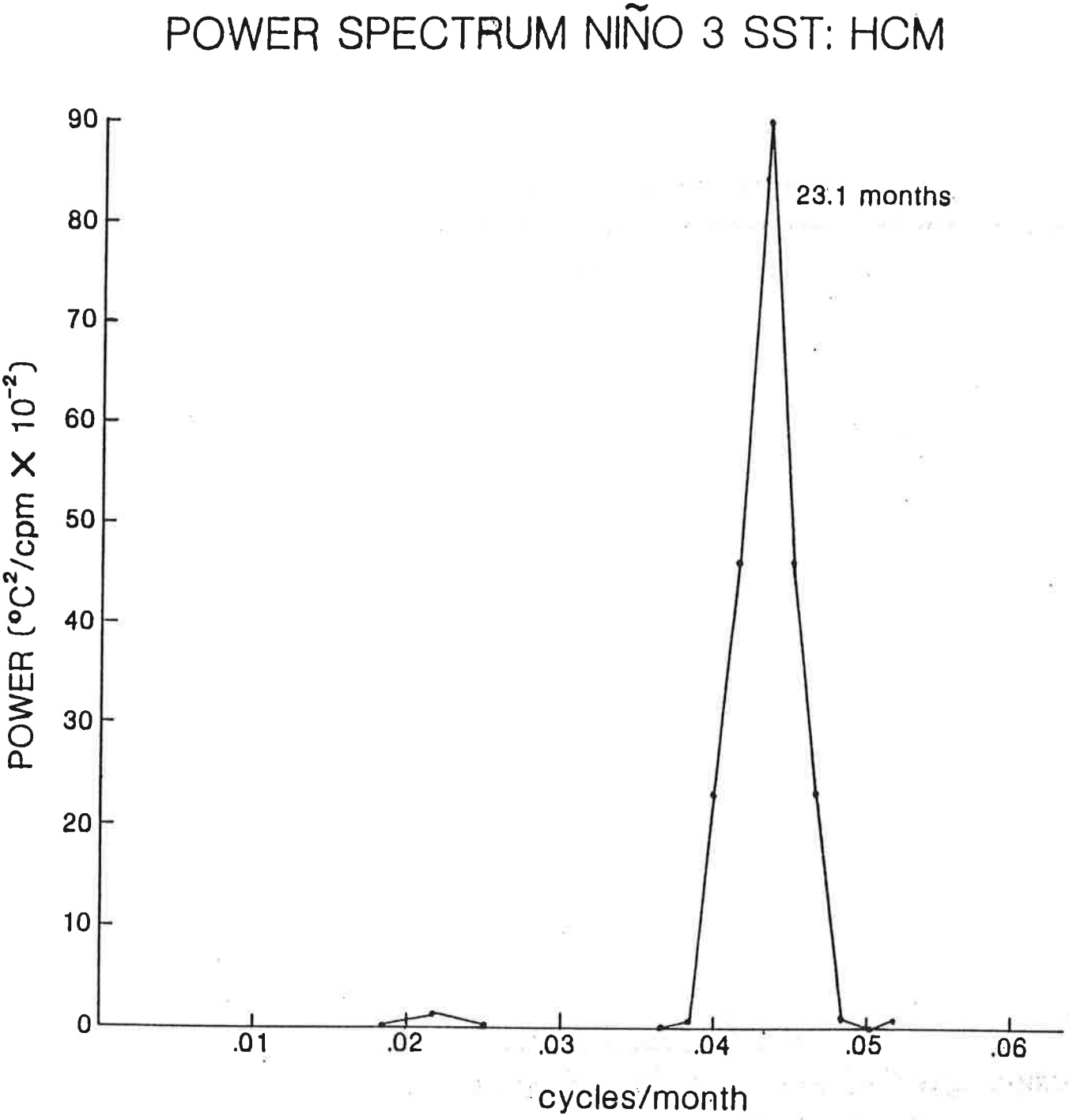

Fig. 7. Power spectrum of NINO3 SST anomaly from 50-year run of the Hybrid Coupled Model. The peak energy is roughly 30 times higher than that obtained by stochastic forcing of the same OGCM (ref. Fig. 4).

to 1), one may surmise that the ocean-atmosphere coupling enhances the amplitude of the LF variations by roughly a factor of $\sqrt{30}$ or 5-6.

In summary, the role of air-sea interactions in the LF mode found in the ocean is that of an amplifier. Without this amplification, the role of the LF variations in interannual climate change, e.g., ENSO, would likely be unimportant. In performing the role of amplifier, these same interactions introduce the LF variation into the atmosphere (as described in Section 4), and thus a much larger region of the planet (cf. Barnett, 1991, Figs. 2, 3 and 5).

5.2 The Role of Seasonality

The seasonal cycle does play an important role in the LF variability but, as we have seen above, it is not what one might term a direct role. The role of seasonality in producing the LF variations has been demonstrated by two additional numerical experiments with the HCM. Both runs start from a comparable, but not identical, initial condition (t_0) obtained from, say, July of a control run. In the first experiment, the integration was allowed to continue beyond t_0, with normal changes in the annual cycle, i.e., the seasonal cycle component of the wind stress was allowed to evolve as appropriate to the time of year. The wind anomalies, however, were computed by the atmospheric model under the assumption of a perpetual July, i.e., there was no seasonality in the atmospheric feedback. In the second experiment, both the seasonal component of the wind and the atmospheric anomaly model were held to July, i.e., a perpetual July was imposed on both the seasonal cycle and the atmospheric feedback.

The results of both experiments are demonstrated clearly by inspecting the time history of SST in region NINO3 (Figure 8) for the first 26 years of the coupled integrations. The comparable time history for the continuation of the control run, which included full seasonality in both the wind stress annual cycle specification and in the coupling coefficients of the anomalous atmospheric model, is shown for comparison.

The LF mode of variability is missing from both altered simulations (upper and middle panels). In its place is a highly regular 5-year oscillation.[1] Inclusion of the seasonal cycle in the specified background mean state (the first experiment, middle panel) did little to affect this finding aside from adding variability at the annual time scale. Allowing for seasonality in the ocean-atmosphere coupling (lower panel) produced irregular and higher frequency

[1] This is one of the characteristic ENSO time scales estimated by other authors, and so represents an interesting result which will be pursued elsewhere.

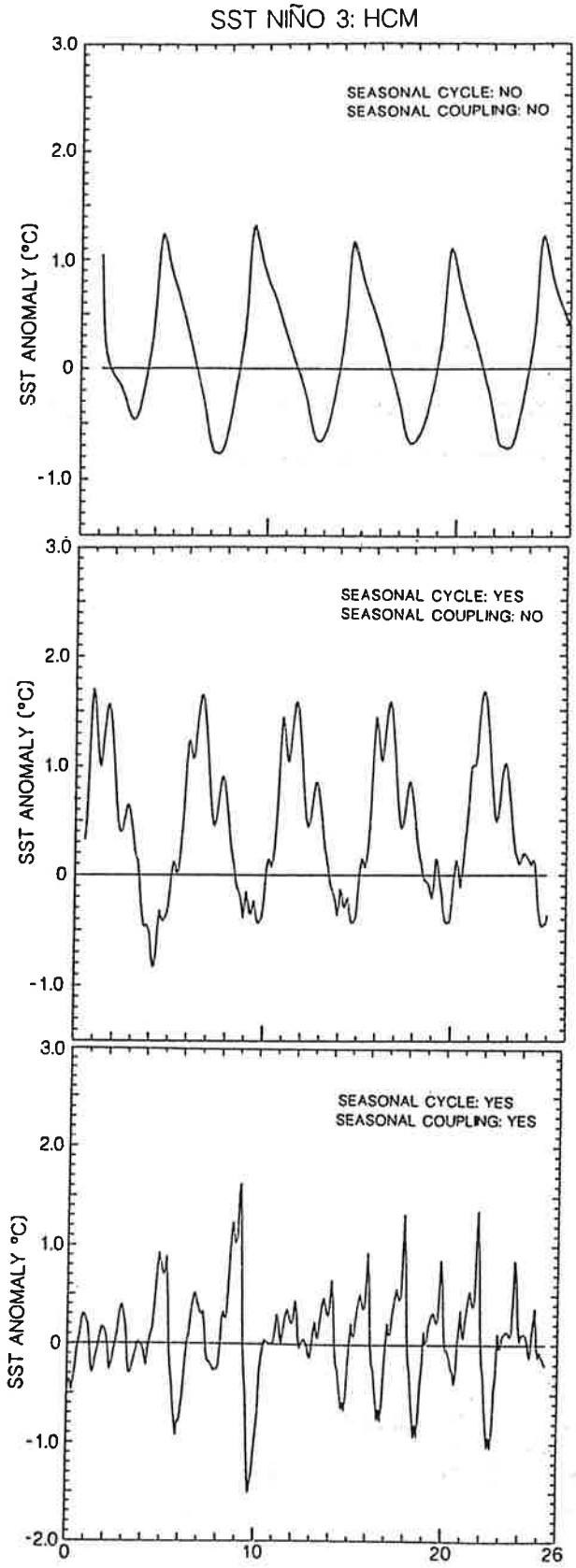

Fig. 8. Time series of NINO3 SST anomaly from HCM runs with various forms of seasonal wind forcing: No seasonal cycle and no seasonal dependence in the anomalous ocean/atmosphere coupling (upper); seasonal cycle forcing from climatology and no seasonal dependence in the anomalous ocean/atmospheric coupling (middle); seasonal cycle forcing from climatology and seasonal dependence in anomalous ocean/atmosphere coupling (lower).

variability. It is clear that in the HCM, at least, the seasonality in the degree of ocean-atmosphere coupling is critical to the existence of the LF variability. The annual cycle, by itself, does not directly participate in the LF.

Brier (1978) and Nicholls (1978, 1984) have suggested that low-frequency variability could be induced by an ocean-atmosphere interaction whose strength (or sign) varied with the annual cycle. In concept, at least, this was also Meehl's (1987, 1992) suggestion. That is exactly the type of mechanism at work in the HCM. Such a mechanism would produce a negligible nonlinear interaction coefficient between the LF and annual cycle as found by Barnett (1991) and in Part I. In summary, the results presented here, plus those reported by earlier workers, support the hypothesis that the LF variability is associated with the seasonally varying manner in which the ocean and atmosphere interact with each other. The interested reader is referred to B93 for a description of the seasonal character in the HCM.

6.0 The Time Scale

In general, the estimates of spatial structure of the LF mode we obtained from the different numerical experiments and observations are rather consistent with each other. However, the temporal variability, as denoted by the estimated period of the LF mode, is more variable than we would have expected *a priori*. There are at least two reasons for this:

i) Estimation error

In a POPs analysis, there are four different ways to obtain the characteristic time scale (see Part I for a description). They can give rather different answers (cf. Fig. 9). For example, the regular POP period and energy weighted phase estimates both gave periods near 40 months while the amplitude weighted cumulative phase method gave 34 months for the observations (Part I). All of these measures are subject to overestimation in the presence of a few large amplitude events (e.g. 1982-83 ENSO). The unweighted cumulative phase estimation procedure, which is unaffected by large magnitude events, gave a period of 27 months. So the POP-estimated time scale for the LF mode lies in the range 27 to 40 months; the range depending solely on analysis method. Note, however, in Fig. 9 the clear temporal separation of the QB and LF modes.

The spectral estimate (from Fig. 4) from the noise forced OGCM run gave a characteristic LF time scale of roughly 27 $\pm$ 1 months while the POP period of that run gave a 29

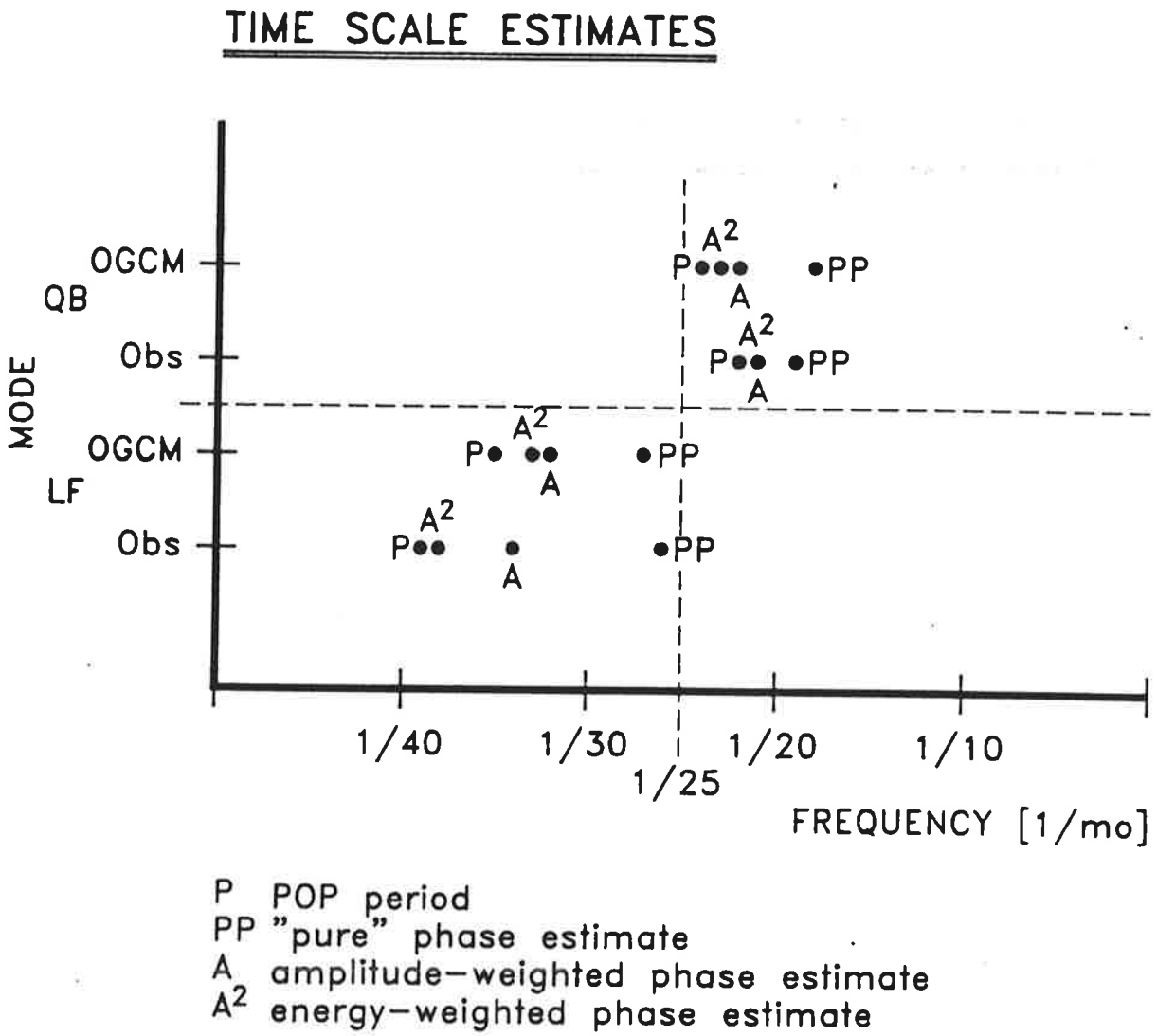

Fig. 9. Time scale estimates for the LF and QB mode by four different methods from the POPs analysis of the observations (OBS) and OGCM forced by the observed winds OGCM. Note the time scale separation of the two modes and the rather good correspondence between like estimates for the observations and simulation. The symbols are defined on the Figure and explained in Part I.

month period. Combining these results with those just above suggests we can assign a time scale of 26-40 months to the LF mode. Note this time span includes what many authors have called the quasi-biennial period (e.g. Trenberth, 1975; Quiroz, 1983; Rasmusson *et al.*, 1990; Yasunari, 1989).

The highly unsatisfactory situation with time scale estimation is due to the fact that the processes we are studying are broadband in frequency space (but apparently highly peaked in wave number space). Without a dominant spectral frequency peak, it seems unlikely that a characteristic time scale can be defined with high precision.

ii) Physical Causes

The mode of oscillation we have described contains a strong element that results from air-sea coupling. The nature and strength of that coupling, in good part, determines the time scale of the oscillation. Each of the sections and/or experiments described above feature a different form of air-sea coupling and all of these differ in turn from the real world (Part I). Perhaps it is surprising that the characteristic time scales estimated above for the observations and variety of model runs are as close to each other as they are.

In summary, the estimation of time scale associated with the LF is not precise. It seems likely that this situation is not only a result of analysis procedures but a characteristic of the natural system.

7.0 Conclusions

A variety of numerical simulations have been carried out in order to investigate the origins of the LF mode described in Part I of this paper. The principal results of this study are as follows:

i) An atmospheric general circulation model (AGCM) forced by observed SST anomalies reproduced remarkably well the LF mode variability found in the sea level pressure and other tropical Pacific fields. The same AGCM forced only by climatology (the seasonal cycle of SST) did not reproduce the observed LF variability. We conclude that the LF mode has its origins in the oceans, not the atmosphere.

ii) An ocean general circulation model (OGCM) was forced with the observed wind stress over a 29-year period. The fields of SST, sea level and wind stress produced patterns of LF variability similar to those found in the data (Part I). It is clear that the OGCM produces reasonably well the spatial and temporal variability in the LF frequency band.

iii) The OGCM was forced by noise that was red in space but white in time. The LF mode described in Part I and ii) above was found in the noise simulations whether or not the seasonal cycle of wind stress or the annual average stress were included. We conclude the variations in the LF mode are largely of oceanic origin and represent a fundamental eigenmode of the tropical ocean. This mode is not dependent directly on seasonal cycle forcing.

iv) A hybrid coupled model (HCM) consisting of the OGCM noted above and a statistical atmospheric component produced spatial LF variations much like those observed in nature and in the run where the OGCM was forced by observed winds. Comparison of this simulation with those described in iii) show that air-sea interactions amplify the LF mode by a factor of 5-6, thereby making it climatologically important. This interaction also essentially introduces LF variability to the atmosphere through the mechanisms described in Barnett *et al.* (1991) and B93.

v) Variability in the LF band depends critically on the seasonality in the strength of the coupling between the ocean and atmosphere. This is distinctly different from the assertion that the LF is driven directly by the annual cycle.

vi) The characteristic time scale one assigns to the LF mode can vary from 26-40 months depending on the analysis procedure one uses. Some of these estimates fall into a range of time scales often associated with the tropospheric quasibiennial oscillation. Given the broadband nature of the frequency spectrum in the range from 1 cycle/20 months to 1 cycle/40 months, it seems unlikely that the time scale of the LF mode can be more precisely determined.

Acknowledgments

Support for this work was provided by the office of Climate Dynamics Program, National Science Foundation under grant NSF ATM88-14571-03, and the Scripps Institution of Oceanography. Thanks are due Tony Tubbs for carrying out most of the calculations required for this paper and to C. Keller of IGPP Los Alamos National Laboratory who made computer time available as part of the University of California's INCOR program.

References

Barnett, T. P., 1983: Interaction of the monsoon and Pacific trade wind system at interannual time scales. Part I: The equatorial zone. *Mon. Wea. Rev.*, **111**, 756-773.

Barnett, T. P., 1985a: Variations in near global sea level pressure. *J. Atmos. Sci.*, **42**, 498-501.

Barnett, T. P., 1985b: Three dimensional structure of low frequency pressure variations in the tropical atmosphere. *J. Atmos. Sci.*, **2**, 2798-2803.

Barnett, T. P., 1991: The interaction of multiple time scales in the tropical climate system. *J. of Clim.*, **4**, 269-285.

Barnett, T. P., N. Graham, M. Latif, S. Pazan and W. White, 1993: ENSO and ENSO-related predictability: Part I: Prediction of equatorial Pacific sea surface temperature with a hybrid coupled ocean-atmosphere model, *J. Clim.*, submitted.

Barnett, T. P., M. Latif, E. Kirk and E. Roeckner, 1991: On ENSO Physics. *J. of Clim.*, **4**, (5), 487-515.

Brier, G. W., 1978: The quasi-biennial oscillation and feedback processes in the atmosphere-ocean-earth system. *Mon. Wea. Rev.*, **106**, 938-946.

Cane, M. A., M. Münnich and S. E. Zebiak, 1990: A study of self- excited oscillations of the tropical ocean-atmosphere. Part I: Linear Analysis, *J. Atmos. Sci.*, **47, (13)**, 1562-1577.

Fischer, G., 1987: Large scale atmospheric modeling. Rep. No. 1, Meteorological Institute, University of Hamburg, West Germany, p. 159.

Goldenberg, S.B. and J.J. O'Brien, 1981: Time and space variability of the tropical Pacific wind stress. *Mon. Wea. Rev.*, **109**, 1190-1207.

Graham, N.E. and W. B. White, 1988: The El Niño / Southern Oscillation as a natural oscillator of the tropical Pacific Ocean-Atmosphere system, *Science*, **240**, 1293-1302.

Latif, M., 1987: Tropical ocean circulation experiments. *J. Phys. Oceanogr.*, **17**, 246-263.

Latif, M., T.P. Barnett, N. Graham, and M. Flügel, 1993: Modal structure of variations in the tropical Pacific climate system, Part I: Observations. *J. Atmos. Sci.*, submitted.

Latif, M., J. Biercamp, H. von Storch, M. McPhaden and E. Kirk, 1990: Simulation of ENSO related surface wind anomalies within an atmospheric GCM forced by observed SST. *J. Clim.*, **3**, 509-521.

Meehl, G. A., 1987: The annual cycle and its relationship to interannual variability in the tropical Pacific and Indian Ocean regions. *Mon. Wea. Rev.*, **115**, 27-50.

Meehl, G. A., 1992: A coupled air-sea biennial mechanism in the tropical Indian and Pacific regions: Role of the ocean, *J. Clim.*, in press (Nov., 1992).

Miller, A. J., T. P. Barnett and N. Graham, 1992: A comparison of some tropical ocean models: Hindcast skill and El Niño evolution. *J. Phys. Oceanog.*, submitted.

Nicholls, N., 1978: Air-sea interaction and the quasi-biennial oscillation. *Mon. Wea. Rev.*, **106**, 1505-1508.

Nicholls, N., 1984: The Southern Oscillation and Indonesian sea surface temperature. *Mon. Wea. Rev.*, **112**, 424-432.

Philander, S.G.H., 1990: A review of simulations of the Southern Oscillation. International TOGA Scientific Conference Proceedings, Honolulu, Hawaii, 16-20, July, 1990. World Climate Research Programme, WCRP-43, WMO/TD-No. 379.

Phillips, O. M., 1962: On the generation of waves by turbulent wind. *J. Fluid Mech.*, **2**, (5), 417-445.

Quiroz, R.S., 1983: Relationships among the stratospheric and tropospheric zonal flows and the Southern Oscillation. *Mon. Wea. Rev.*, **111**, 143-154.

Rasmusson, E. M., X. Wang and C. F. Ropelewski, 1990: The biennial component of ENSO variability. *J. Mar. Sys.*, **1**, 71-90.

Ropelewski, C.F., M.S. Halpert, and X. Wan, 1992: Observed tropospheric biennial variability and its relationship to the Southern Oscillation, *J. Clim*, **5(6)**, 594-614.

Sausen, R. (ed)., 1991: Studying climate with the atmospheric model ECHAM. Report 9. Met. Inst., U. Hamburg, D-2000, Hamburg, Germany, pp. 187.

Schopf, P. S., and M. J. Suarez, 1988: Vacillations in a coupled atmosphere-ocean model, *J. Atmos. Sci.*, **45**, 549-566.

Trenberth, K. E., 1975: A quasi-biennial standing wave in the Southern Hemisphere and interrelations with sea surface temperature. *Quart. J. Roy. Meteor. Soc.*, **101**, 55-74.

von Storch, 1988: Climate simulations with the ECMWF T-21 Model in Hamburg, p. 265. [Available from Meteorological Institute, University of Hamburg, Hamburg, Germany.]

Yasunari, T., 1989: A possible link of the QBO's between the stratosphere, troposphere, and sea surface temperature in the tropics. *J. Meteorol. Soc. Japan*, **67**, 483-493.